



# VERTICAL PROFILES OF STREAMWISE VELOCITY INSIDE NON- AND VEGETATED MEANDERING COMPOUND CHANNEL

Abdul Haslim Abdul Shukor Lim, Zulhilmi Ismail, Mohamad Hidayat Jamal and Mazlin Jumain  
Department of Hydraulics and Hydrology, Faculty of Civil Engineering, Universiti Teknologi Malaysia, UTM Skudai,  
Johor, Malaysia

E-Mail: [haslim1554@gmail.com](mailto:haslim1554@gmail.com)

## ABSTRACT

Advances in computer capabilities have increased the interest of using more complex simulation model into solving the Navier Stokes equation in open channel. Computational fluid dynamics using Large Eddy Simulation model were used to simulate the vegetation presence on floodplain along main channel inside meandering compound channel. Simulations were done for two different relative depths for non- and vegetated cases. The measured and predicted inbank streamwise velocity were compared at bend apex of the compound channel for validation. Presence of vegetation significantly reduces the velocity in the area near the vegetated main-channel and floodplain interface also in the area protected from the upstream flows. The numerical result shows that the flows inside the main channel were greatly affected by the vegetation especially for low relative depth. Interaction between streamwise velocity of overbank and inbank becomes more complex thus highly turbulence in the area near the vegetation.

**Keywords:** meandering compound channel, vegetation, large eddy simulation, three-dimensional, overbank.

## 1. INTRODUCTION

In recent years, meandering compound channels have been considered as one of the approaches that provide a balance between environmental, economic, ecology, aesthetic and amenity values. Thus, capable tools in predicting the flow processes in such channels are requires. TELEMAC-3D, a three-dimensional computational fluid dynamics tools were used to simulated the flows conditions inside meandering compound channel with the presence of vegetation along the main channel.

TELEMAC-3D is a finite element model that comes with solution module using Large Eddy Simulation method to solve the filtered three-dimensional Navier-Stokes equations using prismatic elements build from layers of horizontal unstructured triangular mesh planes. Filtered LES method solves for the larger eddies meanwhile the smaller eddies were left unsolved or been modelled by another model such as subgrid-scale model as the most contributions to the Reynolds stresses come from the larger eddies.

The applications of Large Eddy Simulation method in open channel has been widely used with the advanced of computing capabilities as it offers more accurate solutions than Reynolds-averaged Navier Stokes methods. Improved predictions of the complex interaction of turbulence flows were recorded by van Balenet *al.* [1] for simulations using Large Eddy Simulation on meandering and curved channel. Kang and Sotiropoulos [2,3] and Kokenet *al.* [4] were among the others that used Large Eddy Simulation models to simulate meander and curved open channel.

Large Eddy Simulation models also have been applied to simulate flows with emergent and submerged structures that mimicking vegetation by the works of Cui and Neary [5], Stoesseret *al* [6,7], Kim and Stoesser [8], Mattisetet *al* [9] and many more. The model successfully captured the flow separation and reattachment of water column and turbulences induces by these structures or

vegetation. More intense reviews and discussions on the uses of Large Eddy Simulation methods in open channel can be found on the paper written by Stoesser [10].

A physical meandering channel in the Hydraulics and Hydrology Laboratory, UniversitiTeknologi Malaysia were modelled numerically to simulate the flows conditions of vegetated floodplain for different relative depth. The used of three-dimensional computational fluid dynamics model can give better understandings of the interactions between fast moving inbank flows and slow-moving overbank flows inside the compound channel when compared with any others dimensional model approach due to the strong-three-dimensional flow behaviour as shown in the works by Ervine *et al* [11] and Shiono and Muto [12].

## 2. THREE-DIMENSIONAL MODELLING OF MEANDERING COMPOUND CHANNEL

An existing compound channel with a meander main channel with sinuosity 1.374 and floodplain on both sides at Hydraulics and Hydrology Laboratory, UniversitiTeknologi Malaysia were modelled numerically. The main channel is a 3 and quarter wavelength meander main channel with 50cm wide and 9cm height. Vegetations were placed on the left-hand side floodplain along the main channel starting from 1 and half meander bend apex for a complete one meander wavelength in cases of vegetated flows. Physical measurements were taken at several cross-sections inside the second half of the vegetated meander as shown in Figure-1

Steel rods with diameter of 0.5cm were placed in staggered two-line conditions with a distance of the first line is 5cm from the interface of the main channel and left-hand side floodplain to represents as emergent vegetation. These vegetations were placed at two times the rod diameter from each other. Mesh generation was optimized to save computational time in most of the compound



channel but denser meshes were built around the vegetated area to capture the complex flows near the vegetation.

A total of 12 layers of horizontal planes from the bottom to the free surface with divided equal distances were used to produce the prismatic elements of the three-dimensional meshes inside the compound channel. The number of the horizontal planes were kept between over-discretised on the floodplains and under-discretised in the main channel as over-discretised will increase the computational times while under-discretised model will prevent accurate flow predictions inside the main channel.

The computational cases were simulated for two different relative depth of overbanks flows of 0.30 and 0.45 for non- and vegetated floodplain. The details of the computational properties are shown in Table-1. The relative depth, DR of the overbank flows can be calculated using:

$$DR = \frac{H - h_{mc}}{H} \quad (1)$$

where,  $H$  is total water depth and  $h_{mc}$  is depth of main channel.

Selected vertical profiles of the normalised streamwise velocity at four points on the floodplain and two in the main channel at every measurement sections are presents in this paper. Points selections based on location criticality and the limitations of Acoustic Doppler Velocitimeter to measure those locations. Details location of the points were shown in Figure-2 with point A is at 0cm, point B at 12cm, Point C at 16cm, Point D at 22cm, Point E at 68cm and Point F at 90cm at each measuring sections. Point A and Point F are on the floodplains with a distance of 20cm from the main channel and floodplains interface. Point B and Point C is on the left-hand side floodplain with a distance of 1.5cm and 1 cm from the vegetation while Point D and Point E are inside the main channel with distances of 2cm from the interface.

Initial and boundary conditions were predetermined to closely represent the actual uniform flows in the experiments. Simulated models were calibrated using the roughness coefficient until the water surface profile to be parallel as the channel bed gradient to closely resemble the uniform flows conditions that being modeled. Calibrated model than further validated by the measured streamwise velocity at bend apex through the available data from studies done by Ibrahim [13].

Streamwise velocity were normalised to the sectional-average velocity,  $U_s$  where  $U_s = Q/A$  for better comparisons between both relative depth.  $Q$  is the discharge and  $A$  is the cross-sectional area at bend apex. Normalised streamwise velocity of the inbanks were presented by water level below zero. Further explanations and elaborations on the computational sequence can be found in details by the works of Sukla [14].

### 3. RESULTS AND DISCUSSIONS

#### 3.1 Validation

Validations for the simulations cases were shown in Figure-3. Validation of DR 0.45 for non-vegetated and vegetated cases has been done by comparing the streamwise velocity of the measured and the predicted at the centre of the main channel at measurement Section 1. Same validation also was done for DR 0.30 at the centre of the bend apex main channel but at a different measurement cross-section of Section 15.

#### 3.2 Vertical profiles of streamwise velocity

Figures 4 to 5 shows the vertical profiles of the normalised streamwise velocity on the floodplains and inside the main channel of non-vegetated and vegetated for both DR cases. Inbank flows inside the main channel represents by water level (WL) below zero and overbank flows by water level above zero. In general, the vertical profiles of non-vegetated cases generated the same patterns for both relative depths even though some discrepancy was recorded at some points in the measurement sections. These similarities were also recorded by vegetated cases of both relative depths on the floodplains and inside the main channel. The most significant discrepancy of the streamwise velocity was recorded at Point E of measurement Section 8 inside the main channel where the cross-over of overbank flows take place.

Magnitudes of the normalised streamwise velocity inside the compound channel that follows the direction of the compound channel were higher for vegetated cases rather than the non-vegetated cases for the same relative depth. Meanwhile, the normalised streamwise velocity inside the area on the left-hand side floodplain that being protected from upstream overbanks flows by vegetation were smaller for both vegetated cases. In some locations likes Point C at measurement Section 1 and Section 15, the streamwise velocity were almost in stalemated conditions and some even in backward direction from upstream flows of the compound channel were recorded. This change of directions of streamwise velocity to backward or negative values were due to the vortex phenomenon that generated near the vegetation. Vortex was known to produce from the momentum transfer of fast-moving flows of in the main channel into slow-moving flows on the floodplains, the effects that clearly visible in a straight compound channel.

Significant reductions of normalised streamwise velocity were recorded at almost all points on the left hand side floodplain but not true for Point A and Point B at bend apex measurement Section 1. The highest reduction on the left-hand side floodplain were recorded at Point A for DR 0.30 and Point B for DR 0.45 of measurement Section 15. Maximum reduction of 94.9% for DR 0.30 and 92.9% for DR 0.45 on Point A meanwhile, change of direction from the upstream flows for Point B were recorded for both of the vegetated cases. These reduction patterns of streamwise velocity on the left-hand side floodplain were not true for Point A and Point B at bend



apex measurement Section 1. In these locations, streamwise velocity for vegetated cases increased up to 45.6% for DR 0.30 and up to 34% for DR 0.45 when compared to the non-vegetated cases of the same relative depth.

Increasing magnitudes of the streamwise velocity patterns in lower half of the overbank flows were spotted at Point C for measurement Section 4, Section 8 and Section 12 but start to decrease in the upper half of the overbank flows. These increases of velocities were due to the effect of higher inbank velocities inside the main channel to the overbank flows near the interface. Meanwhile, the decreasing streamwise velocity patterns in the upper half were due to the increase of resistance by the vegetation to the overbank flow. The effects of fast-moving inbank flows only significant to the lower part of the overbank flows before the presence of vegetation overtakes their role in the upper part of the overbank flows in the area near the vegetated main channel-floodplain interface. Nearly unmoving streamwise flows conditions were recorded on Point C at measurement Section 1 due to the protection given by the vegetation along the meander main channel.

Normalised streamwise velocity vertical profiles near the interface inside the main channel are shown by Point D and Point E. Inbank streamwise velocity on Point D were greatly affected by the presence of the vegetation for both relative depths. Significant reduction of the inbank flows can be seen at bend apex measurement Section 1 but it starts to increase at measurement Section 8 as it goes downstream till the next bend apex of measurement Section 15. The velocities decreased were up to 83.3% for DR 0.30 and 72.2% for DR 0.45 at measurement Section 1 of the inbank flows. The highest increase of streamwise velocity for inbank flows was recorded at the cross-over region of measurement Section 8 for both Point D and Point E. The velocity increased is 3.2 times for DR 0.30 and 4 times for DR 0.45 in the location near the vegetated main channel-left-hand side floodplain interface.

Vegetation greatly reduced the streamwise velocity of overbank flows in the main channel especially on Point D that located near the vegetation. In this location, the dominant of fast-moving inbank flows increased the magnitude of the overbank flows but becomes less significant as streamwise velocity approach the free surface. These reduction patterns were not true at measurement Section 15 where in this section, directed overbank flows by the vegetation has increased the

magnitude of the overbank flows passing through this section.

The effect of vegetation to overbank streamwise flows on Point E becomes less significant at measurement Section 12 and Section 15, therefore the vertical profile patterns start to closely resemble the cases without vegetation. Still, the increase of inbank flows magnitude were recorded on Point E at measurement Section 1, Section 4 and Section 8 of the vegetated cases for both relative depths. Vegetation on left-hand side floodplain has minimum effects towards the overbank flows on the right-hand side floodplain represents by Point F except at bend apex

#### 4. CONCLUSIONS

Inbank flows of vegetated floodplain case for low relative depth was greatly affected by the presence of vegetation along the main channel especially inside the cross-over regions where the highest increased of streamwise velocity was recorded. Protections given by vegetation increased the influence of fast-moving inbank flows towards overbank flows inside the main channel but it starts to losses it influences as the overbank flows downstream towards the unprotected by vegetation bend apex of the meandering compound channel. Vegetation along the main channel greatly reduces the quantities of conveyance of the overbank flows crossing over to the vegetated floodplain, thus, diverts most of the overbank flows to follows the direction of the main channel. Protection and flows diversion by vegetation significantly reduced the velocities in the area near the vegetation and in the area protected from the upstream flows inside the compound channel. Reductions of streamwise velocity also indicated significant losses of energy build inside the meandering compound channel.

Vegetation on the floodplain along the main channel also disrupts one of the important phenomenon inside meandering compound channel, the contraction and expansions of overbank flows inside the cross-over regions, thus significantly affects the generated turbulence from this phenomenon that critical for the secondary flows circulations inside the meander main channel. These interruptions making the interactions between the overbank and inbank flows becomes more highly turbulence and complex than they already were. Changes in velocities especially near the interface also have major significant relationship to the boundary shear stress, one of the important factor behind erosion and sedimentation.

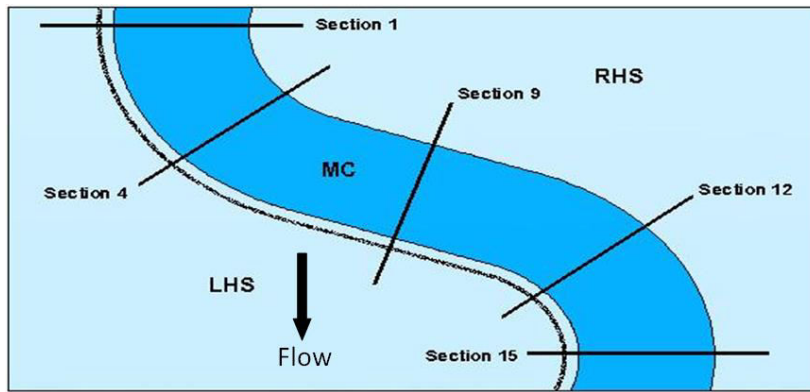


Figure-1. Measurements sections on meandering compound channel.

Table-1. Simulation properties.

Case	Discharge, Q (l/s)	Water depth, H (cm)	Relative depth, DR	Manning's, n	Sectional -average velocity, $U_s$ (cm/s)	Total nodes	Total elements	No. of horizontal planes	Time step, t (s)
NV DR0.30	38.0	12.86	0.30	0.0142	23.6	274980	464706	12	0.01
NV DR0.45	85.0	16.36	0.45	0.0180	28.1	274980	464706	12	0.01
2D DR0.30	30.0	12.86	0.30	0.0190	18.7	1041912	1827496	12	0.0075
2D DR0.45	48.7	16.36	0.45	0.0320	18.3	1041912	1827496	12	0.0075

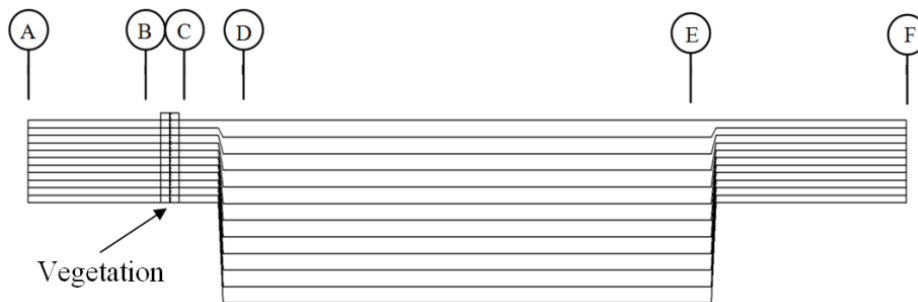


Figure-2. Vertical profile locations in measurement sections.

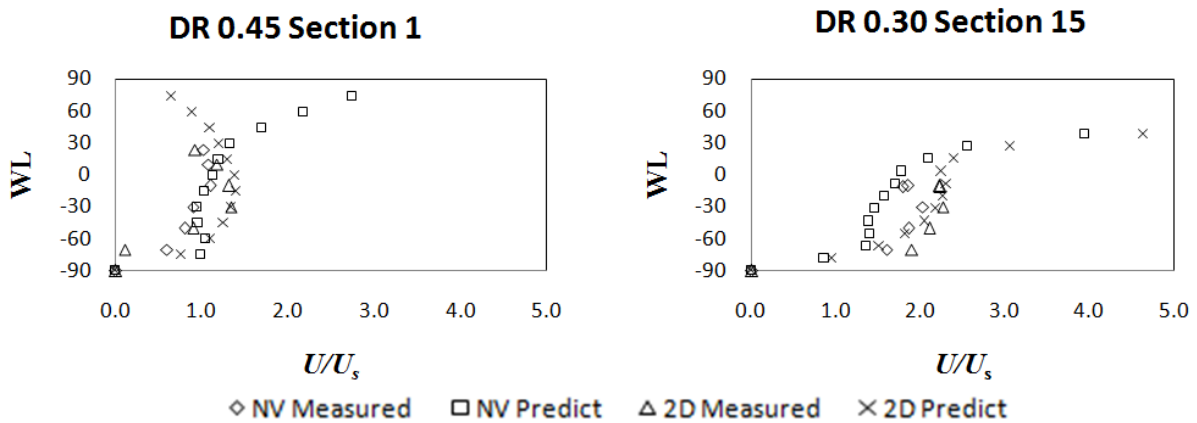
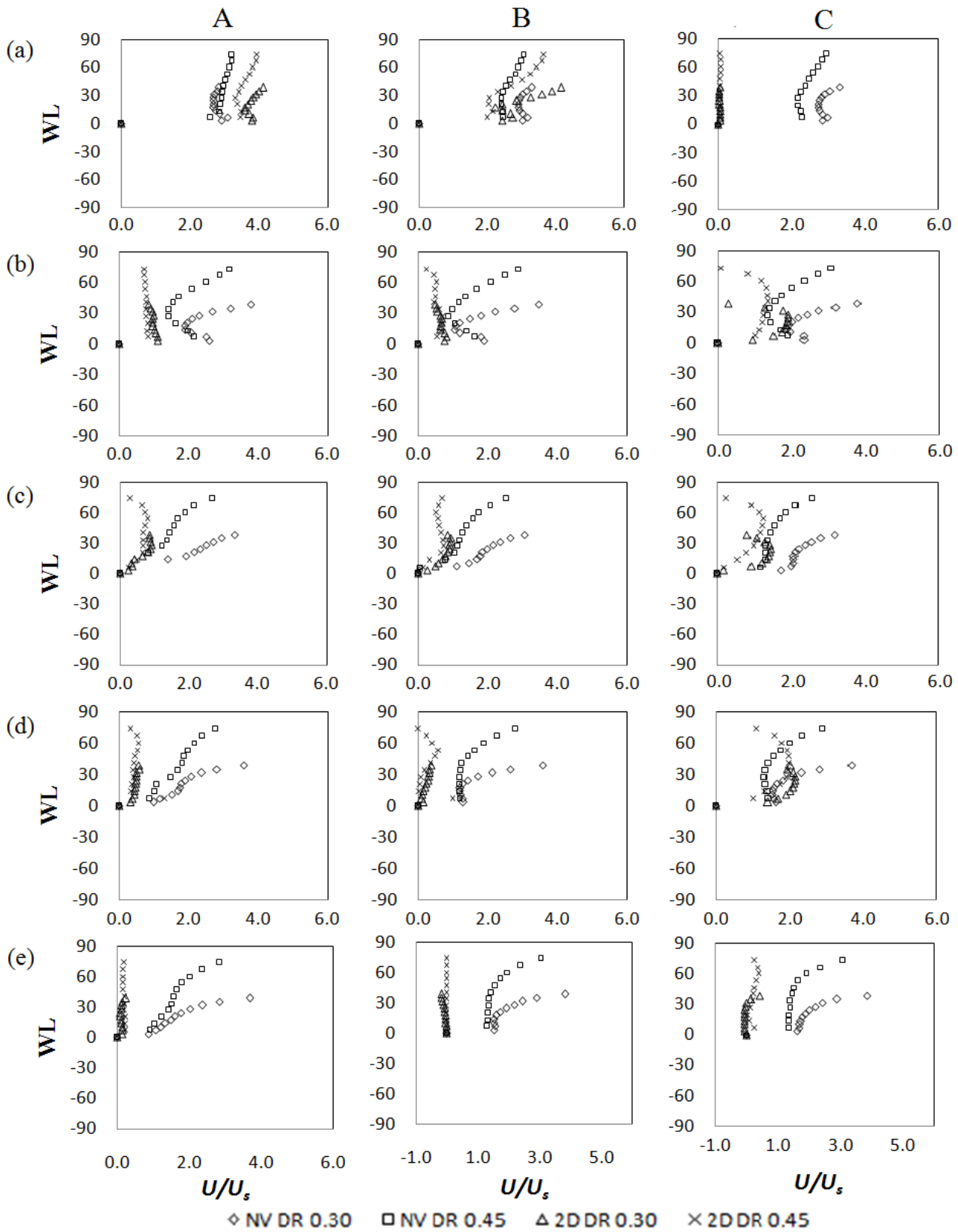
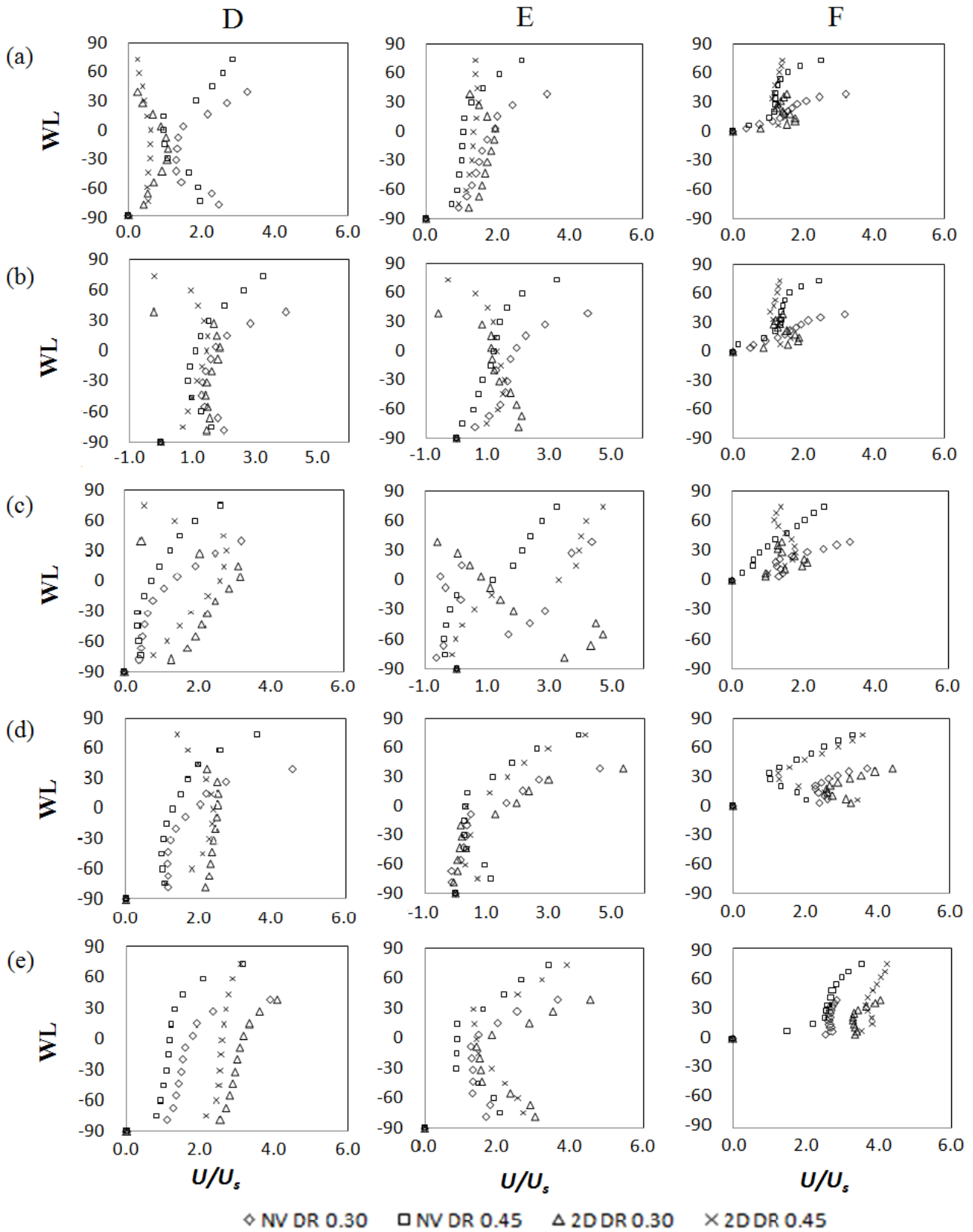


Figure-3. Normalised streamwise velocity vertical profile centre of the main channel at a) Section 1 DR 0.45 and b) Section 15 DR 0.30 for non- and vegetated meandering compound channel.



**Figure-4.**  $U/U_s$  vertical profile at Point A (0cm), Point B (12cm) and Point C (14 cm) at a) Section 1; b) Section 4; c) Section 8; d) Section 12; and e) Section 15 of non-vegetated and vegetated cases for DR 0.30 and DR 0.45.





**Figure-5.**  $U/U_s$  vertical profile at Point D (22cm), Point E (68cm) and Point F (90 cm) at a) Section 1; b) Section 4; c) Section 8; d) Section 12; and e) Section 15 of non-vegetated and vegetated cases for DR 0.30 and DR 0.45.

**ACKNOWLEDGEMENT**

Authors would like to express the highest gratitude to Faculty of Civil Engineering, UTM for funding and providing their facilities for this research respectively.

**REFERENCES**

- [1] VanBalen W., Uittewaal W. S. J. and Blanckaert K. 2010b. Large eddy simulation of a curved open-channel flow over topography. *Physics of Fluids*. 22, 075108.
- [2] Kang S. and Sotiropoulos F. 2011. Flow phenomenon and mechanism in a field-scale experimental meandering stream with a pool-riffle sequence: Insight gained via numerical simulation. *Journal of Geophysical Research*. 116, F03011.
- [3] Kang S. and Sotiropoulos F. 2012a. Numerical modelling of 3D turbulent free surface flow in natural waterways. *Advances in Water Resources*. 40: 23-36.
- [4] Koken M., Constantinescu G. and Blanckaert K. 2013. Hydrodynamic processes, sediment erosion mechanisms, and Reynolds-number-induced scale effects in an open channel bend of strong curvature with flat bathymetry. *Journal of Geophysical Research*. 118(4): JF002760.
- [5] Cui J. and Neary V. S. 2008. LES study of turbulent flows with submerged vegetation. *Journal of Hydraulic Research*. 46(3): 307-316.
- [6] Stoesser T., Palau - Salvador G. and Rodi W. 2009. Large eddy simulation of turbulent flow through submerged vegetation. *Transport in Porous Media*. 78(3): 347-365.
- [7] Stoesser T., Kim S. J. and Diplas P. 2010a. Turbulent flow through idealized emergent vegetation. *Journal of Hydraulic Engineering*. 136(12): 1003-1017.
- [8] Kim S. J. and Stoesser T. 2011. Closure modelling and direct simulation of vegetation drag in flow through emergent vegetation. *Water Resources Research*. 47, W10511.
- [9] Mattis S. A., Dawson C. N., Kees C. E. and Farthing M. W. 2012. Numerical modelling of drag for flow through vegetated domains and porous structures. *Advances in Water Resources*. 39: 44-59.
- [10] Stoesser T. 2014. Large - eddy simulation in hydraulics: Quo Vadis. *Journal of Hydraulic Research*. 52(4): 441-452.
- [11] Ervine D. A., Willetts B. B., Sellin R. H. J. and Lorena M. 1993. Factors affecting conveyance in meandering compound flows. *Journal of Hydraulics Engineering*. 119(12): 1383-1399.
- [12] Shiono K. and Muto Y. 1998. Complex flow mechanisms in compound meandering channels with overbanks flow. *Journal of Fluid Mechanics*, 376: 221-261.
- [13] Ibrahim Z. 2015. Flow behaviour due to floodplain roughness along riparian zones in compound channels, PhD thesis, Universiti Teknologi Malaysia, Malaysia.
- [14] Sukla, D. R. 2006. Three-dimensional computational investigations of flows mechanisms in compound meandering channels, PhD thesis, Loughborough University, U.K.